THE EFFECT OF PHASE TRANSFORMATION ON THE TENSILE FRACTURE OF AUSTENITIC STAINLESS STEEL

Sergio N. Monteiro* and Heliane Fonseca**

INTRODUCTION

High ductility can be associated with high strength in austenitic steels undergoing phase transformation during plastic straining, and this has been studied extensively in TRIP [1 - 5], high chromium [6], and stainless steels [7, 8]. Bressanelli and Moskowitz [7] suggested that the amount of martensite formed during necking in austenitic steel would enhance ductility, while Rosen et al [8] argued that it was not the total amount of martensite, but its distribution which was important in governing the ductility of the material. Fatigue crack propagation has also been studied in austenitic stainless steel [9, 10], and the crack growth rate was found to be relatively low when martensite was produced at the crack tip [10].

Recently, some fractographic analyses have been reported of TRIP steels [11] and metastable austenitic stainless steel [12]. In high nickel TRIP steel with varying carbon contents, Maxwell [11] found that failure was strongly dependent on the presence of both strain-induced and stress-assisted martensite, and suggested that the mechanisms of failure were (a) cleavage across the stress-assisted martensite plates, and (b) decohesion at the interfaces between austenite and strain-induced martensite, with subsequent void formation. Maxwell also suggested that dispersed carbides in TRIP steels, could initiate strain-induced martensite, and that subsequently voids would initiate at these sites, so preventing the intergranular fracture observed when the martensite initiates at grain boundaries. Working with a relatively highly metastable austenitic stainless steel, Fonseca and Monteiro [12] observed different fracture modes in the temperature range M_s-M_d, ductile fracture being observed at 77K, while predominantly brittle features were seen at higher temperatures.

The study reported here was made with the objective of providing comparative fractographic information concerning the tensile fracture surfaces of a stable and metastable austenitic stainless steel.

EXPERIMENTAL PROCEDURE

The steels were received in the form of extruded bars, and their chemical analysis is given in Table 1. They were annealed for one hour at 1370K to average grain sizes of 31 μm for the Type 302 alloy, and 37 μm for the Type 310 alloy. The annealed structure showed a dispersion of round inclusions with some tendency to align themselves parallel to the longitudinal axis of the bars.

* Department of Metallurgy, Federal University of Rio de Janeiro, Brazil.
** Industrial Technology Secretariat, STI-MIC, Rio de Janeiro, Brazil.

Cylindrical tensile specimens having a gage diameter of 4mm were strained at 77K, 193K, 273K and 298K, under a constant strain rate of 4.2×10^{-4} s^{-1}. In the type 302 alloy no spontaneous transformation was detected at the liquid nitrogen test temperature. In the stable Type 310 alloy, no strain-induced martensite could be detected, either by X-rays or magnetic balance in the specimens fractured at all testing temperatures.

RESULTS

The true stress-true strain curves for both steels are shown in Figure 1. At all temperatures the ductility measured by the strain to fracture is high (> 30%) being greater for the stable 310 steel at low temperatures. Due to the martensitic transformation a greater work hardening rate is developed above 10% strain in the 302 steel as depicted in Figure 1. The typical variation of the work hardening rate with strain for both steels is exemplified in Figure 2 for the 193K test condition. The strain dependence of the volume fraction of martensite is given in Figure 3 for the metastable 302 alloy. Although a greater amount of martensite is developed at 77K, the rate of formation of martensite, $dV/d\varepsilon$, at the beginning of necking is higher at 193K, 273K and 287K as may be seen from Figure 3.

Fracture of Type 310 Alloy

At all four temperatures used, the fracture surfaces of the type 310 alloy presented a general cup-and-cone appearance. Dimples and microvoids, typical of ductile fracture, were the predominant features. The principal mechanism of failure appeared to be intergranular fracture, Figure 4, associated with a pattern of cracks in the central area of rupture. At 273K and 298K, a dispersion of relatively large holes, some containing inclusions, was observed as illustrated in Figure 5, and these correspond in size to the particles detected by optical metallography.

Fracture of Type 302 Alloy

With the exception of the specimens tested at 77K, the fractured specimens of the metastable stainless steel have a generally brittle and neckless appearance, as shown in Figure 6. In particular, at 193K, the fracture surface was covered with craters formed at inclusions or holes enveloped by "packets" of martensite, as shown in Figure 7. Even though metallographic evidence exists for stress-assisted martensite at 77K and 193K, there was no sign of banding [11] which would be attributed to large martensite plates. The features which relate to martensite were always in the form of thin lamellae, typical of strain-induced martensite. At higher temperatures, 273K and 298K, the fracture surface showed cleavage facets and martensite lamellae giving a generally brittle appearance, Figure 8. In spite of this apparently brittle fracture, the uniform elongation was high, Figure 1, which indicates the large effect of phase transformation on the ductility of this material. Contrary to what was observed in the stable 310 alloy, the fracture morphology of the metastable Type 302 did not show signs of intergranular failure when the fracture occurred in this brittle mode.

At 77K, the fracture of the Type 302 alloy was essentially different from those occurring at higher temperature. The surface had a cup-and-cone appearance, with ductile dimples and microvoids as shown in Figure 9.

Failure appeared to be associated with cracks developed at a few areas showing martensite lamellae and cleavage facets.

DISCUSSION

The present fractographic analysis has shown that there is a considerable difference between the modes of fracture of a stable stainless steel and of a metastable one. To some extent this is surprising, since both steels have about the same elongation to fracture (see Figure 1) particularly at 273K and 298K. The stable 310 alloy failed at all temperatures in a ductile fashion. This appears to be a consequence (see Figure 2) of the uniform, slow decrease in work hardening rate with strain. The intergranular mode of rupture, Figure 4, is possibly related to inclusions (see Figure 5) at the grain boundaries. The tensile failure of type 302 alloy indicates a significant influence of phase transformation on its modes of fracture. The rate of formation $dV/d\varepsilon$, the amount [7] and distribution [8] of martensite are responsible for the increase in work hardening rate, Figure 2, and consequently the high ductility observed [12]. Moreover, the specific values of $dV/d\varepsilon$ at the beginning of necking for each temperature led to the differences in modes of fracture. At 77K, Figures 1 and 3, the transformation had reached an almost saturated condition before necking started. Fracture then took place in a ductile manner with the existing martensite apparently helping in the nucleation and propagation of cracks. At 193K and above, strain-induced martensite occurring at the maximum load relates to an effective blocking of necking and to the brittle appearance of the fracture surface in Figure 6. At these temperatures $dV/d\varepsilon$ (see Figure 3) at the maximum load was greater than at 77K, saturation not having been reached. The mechanism proposed by Maxwell [11] of decohesion of the strain-induced martensite lamellae interfaces from the austenite matrix, appears to be the cause of failure under these conditions. Moreover, as also suggested by Maxwell, the strain-induced martensite probably nucleates at inclusions, which would account for the "packets", Figure 7, observed extensively at 193K and to a smaller extent at the higher temperature. Finally, the complex nature of the martensitic transformation under these conditions does not allow a simple analysis of the stresses and strains during necking that could enable a precise characterization of the local failure for each steel and temperature studied.

ACKNOWLEDGEMENTS

This work was partially supported by FINEP, CNPq, CEPG and CNEN. The authors which to thank I. Le May for his invaluable help.

REFERENCES

1. ZACKAY, V. F., PARKER, E. R., FAHR, D. and BUSCH, R., Trans. ASM, 60, 1967, 252.
2. GERBERICH, W. W., HEMMINGS, P. L. and ZACKAY, V. F., "Fracture", P. L. Pratt, Editor, Chapman and Hall, London, 1969, 288.
3. CHANANI, G. R., ZACKAY, V. F. and PARKER, E. R., Met. Trans., 2, 1971, 133.
4. GERBERICH, W. W., HEMMINGS, P. L. and ZACKAY, V. F., Met. Trans., 2, 1971, 2243.
5. BHANDAKAR, D., ZACKAY, V. F. and PARKER, E. R., Met. Trans., 3, 1972, 2619.

6. FAHR, D., Met. Trans., 2, 1971, 1883.
7. BRESSANELLI, J. P. and MOSKOWITZ, A., Trans. ASM, 59, 1966, 223.
8. ROSEN, A., JAGO, R. and KJER, T., J. Mat. Sci., 7, 1972, 870.
9. BATHIAS, C. and PELLOUX, R. M., Met. Trans., 4, 1973, 1265.
10. PINEAU, A. G. and PELLOUX, R. M., Met. Trans., 5, 1974, 1103.
11. MAXWELL, P. C., Metallography, 9, 1976, 9.
12. FONSECA, H. and MONTEIRO, S. N., "Fracture Modes of 302 Stainless Steel under Metastable Conditions", Second International Conference on Mechanical Behaviour of Materials, Boston, August, 1976.

Table 1 Chemical Analysis of Steels Used (Weight Percent)

AISI Type	C	Si	Mn	P	S	Cr	Ni	Mo
302 (metastable)	0.10	0.54	0.74	0.032	0.010	16.7	8.3	0.28
310 (stable)	0.09	0.41	1.84	0.024	0.018	25.8	19.1	0.30

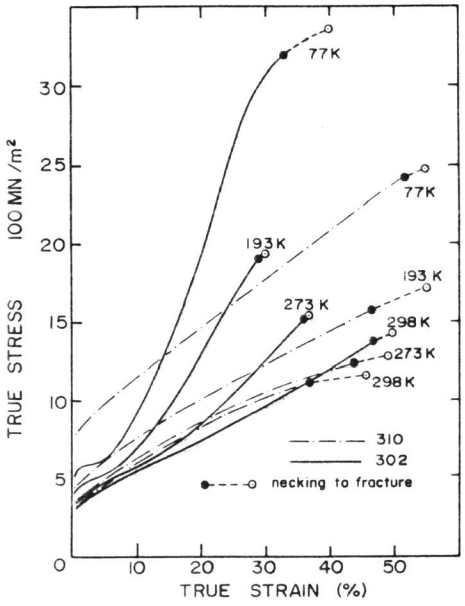

Figure 1 True Stress - True Strain Curves for Types 302 and 310 Alloys

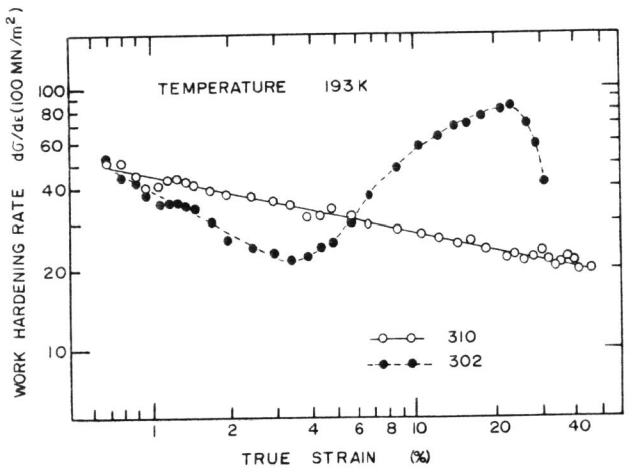

Figure 2 Example of the Strain Dependence of the Work Hardening Rate for Types 302 and 310 Alloys

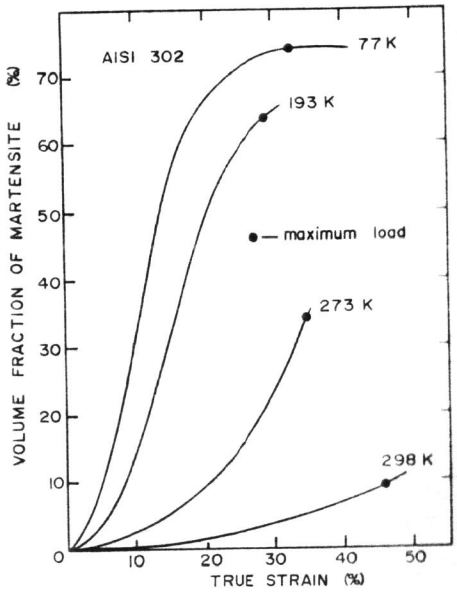

Figure 3 Variation of the Volume Fraction of Martensite up to the Point of Maximum Load in Type 302 Alloy for the Temperatures Investigated

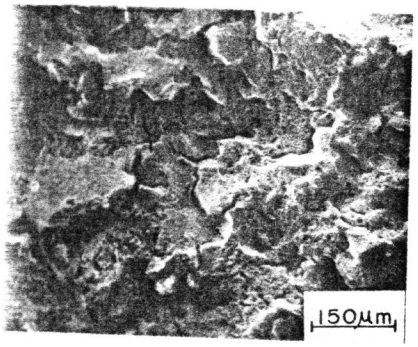

Figure 4 SEM Micrograph of Type 310 Alloy Tested at 193K

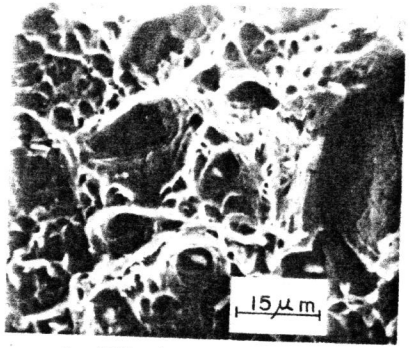

Figure 5 SEM Micrograph of Type 310 Alloy Tested at 298K

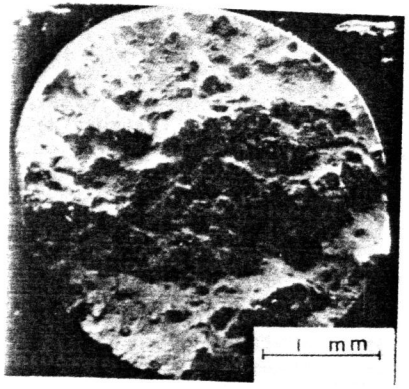

Figure 6 SEM Micrograph of Type 302 Alloy Tested at 193K Displaying General Aspects

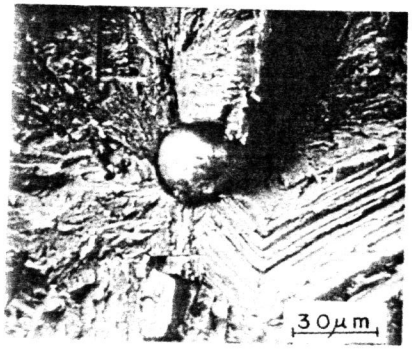

Figure 7 SEM Micrograph of Type 302 Alloy Tested at 193K Showing "Packets" of Martensite Around Inclusion

Figure 8 SEM Micrograph of Type 302 Alloy Tested at 273K

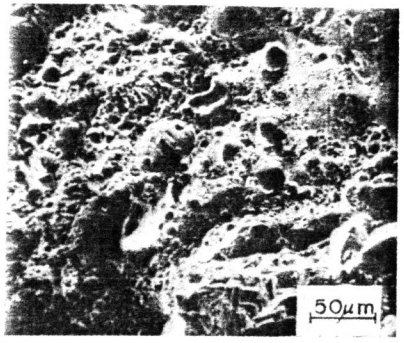

Figure 9 SEM Micrograph of Type 302 Alloy Tested at 77K